Synthesis and Characterization of Superhydrophobic Wood Surfaces

Chengyu Wang,[1] Cheng Piao,[2] Cran Lucas[3]

[1]*College of Materials Science and Engineering, Northeast Forestry University, Harbin, Heilongjiang 150040, People's Republic of China*
[2]*Calhoun Research Station, Louisiana State University Agricultural Center, Calhoun, Louisiana 71225*
[3]*College of Sciences, Louisiana State University at Shreveport, Shreveport, Louisiana 71115*

Received 19 March 2010; accepted 23 May 2010
DOI 10.1002/app.32844
Published online 19 August 2010 in Wiley Online Library (wileyonlinelibrary.com).

ABSTRACT: Superhydrophobic films were developed on wood substrates with a wet chemical approach. Growth of zinc oxide (ZnO) nanorods was found differentially in the cross-sectional walls and inner lumenal surfaces. The surface roughness of the prepared films on the inner lumenal surface conformed to the Cassie–Baxter wetting model, whereas the roughness across the microsurface of the cell wall was in conformity with the hydrophobic porous wetting model. The space between the ZnO nanorods and the microstructure of the wood surface constituted the nanoscale and microscale roughness of the ZnO nanofilm, respectively. The water contact angle of the prepared wood surfaces was up to 153.5°. In the prepared films, monolayers of stearic acid molecules were self-assembled on the ZnO nanorods, which in turn, were attached to the wood surface via dimeric bonds. © 2010 Wiley Periodicals, Inc. J Appl Polym Sci 119: 1667–1672, 2011

Key words: hydrophilic; polymers; metal–polymer complexes; nanocomposites; nanolayers; self-assembly

INTRODUCTION

Unlike metal and some other polymer substrate surfaces, the surface of wood products is soft, uneven, and spotted with pits and debris produced by wood processing tools. Most radial and tangential surfaces of a wood sample consist of concave inner lumenal surfaces with cross-sectional cell walls between them. Depending on the milling location, inner lumenal surfaces of wood cells are commonly intact and are the major components of the radial and tangential surfaces of wood, whereas cell walls between two lumens are longitudinally cut along the cells; this leaves wall cross sections exposed to the air. The alternate concave inner cell wall surface and cell wall cross sections together produce the primary roughness of the wood substrate.

The width of the open lumens and the thickness of cell walls are often variable across the surface of wood products. Depending on the milling location and species, the radius of a tracheid (in softwoods) is 17–60 μm and the radii of a fiber and a vessel (in hardwoods) are 10–30 and 20–350 μm, respectively.[1] Therefore, a 1-mm-diameter water droplet (ca. 4 μL) would cross 17–58 tracheids for softwood and 33–100 fibers or 3–50 vessels for hardwood. Therefore, a local microsurface of wood is often rough. However, a local lumen surface of a wood cell wall is smoother and is often not parallel to the sample surface. Because a nanostructure, such as a nanorod, is often perpendicular to the substrate, a nonuniform orientation of the nanostructure results from the curvilinearity of the local microsurface of the wood. A superhydrophobic surface in such a circumstance is termed a *superhydrophobic porous wetting regime.*[2]

Chemically, wood is composed of celluloses, hemicelluloses, and lignin and can be viewed as a heterogeneous composite. Celluloses and hemicelluloses are carbohydrates, and lignin is a phenolic. All of these substances contain hydroxyls, a molecular group responsible for the cohesion between the architectural building materials of the three major components of the wood cell wall and the adsorption of moisture from the air. Because of the adsorptive nature of the hydroxyl groups, the wood cell wall has the ability to remove water vapor from the surrounding air until it is in moisture equilibrium with the air. Therefore, the chemical transformation of wood from hydrophilicity to hydrophobicity is always associated with the blockage, modification, or removal of the hydroxyl groups on cell walls, which serve to prevent the adsorption of water from the environment.

Correspondence to: C. Piao (cpiao@agcenter.lsu.edu).
Contract grant sponsor: Calhoun Research Station, Louisiana State University Agricultural Center.
Contract grant sponsor: National Natural Science Foundation of China; contract grant number: 30630052.

Extensive studies have been conducted on the chemical modification of wood for hydrophobicity, including acetylation,[3] metal oxide modification,[4] the sol–gel process,[5–7] and microemulsion techniques.[8] These methods can be used to reduce or delay water and moisture sorption of the wood but cannot stop water absorption into the wood by direct contact. Most recently, more hydrophobic surfaces have been developed on fiber surfaces with polymer grafting, layer-by-layer deposition, and plasma treatment.[9–12] However, only a few superhydrophobic surfaces have been developed on solid wood substrates.[13,14]

This study sought to develop superhydrophobic surfaces on wood substrates via a simple wet chemical approach. Zinc oxide (ZnO) nanorods were seeded and grown on the wood cell wall surface. The prepared ZnO nanorod surfaces were then modified with self-assembled monolayers (SAMs) of stearic acid. The prepared hydrophobic surfaces were characterized via scanning electron microscopy (SEM), X-ray diffraction (XRD), Fourier transform infrared (FTIR) spectroscopy, and thermogravimetric analysis (TGA).

EXPERIMENTAL

Southern pine sapwood samples were prepared with a microtome. Each sample was 10 mm wide by 5 mm thick by 60 mm long. The moisture content of the samples was about 8%. The following chemical agents were obtained from Fisher Scientific Company LLC, Houston, TX, or Sigma-Aldrich, Saint Louis, MO, zinc nitrate hexahydrate [$Zn(NO_3)_2 \cdot 6H_2O$], ammonium chloride (NH_4Cl), urea [$(NH_2)_2CO$], ammonia hydroxide (NH_4OH), sodium hydroxide (NaOH), and stearic acid ($C_{17}H_{35}COOH$). All of the chemicals were reagent grade and were used as received.

The synthesis reactions are described as follows. An aqueous solution was prepared in a polytetrafluoroethylene beaker containing 0.01*M* $Zn(NO_3)_2$, 0.01*M* urea, 0.02*M* NH_4Cl, 30 mL of 25% ammonia hydroxide, and 10 mL of 20% NaOH solution. The wood samples were carefully suspended in the solution, which was then heated to 90°C over 25 min. The system was stirred at the same temperature for 20–24 h. The pH of the solution was maintained at 10 ± 0.5 and continuously monitored by a pH meter during the reaction. After the synthesis, the wood substrates were washed with deionized water to remove unreacted chemicals from their surfaces. The substrates were then blown dry with nitrogen for 2 min and were subsequently dried in an oven at 80°C for 24 h.

The SAM coating reaction was conducted in a polytetrafluoroethylene beaker. The treated samples were suspended in an *n*-hexane solution of stearic acid at room temperature for 48 h. After the SAM reaction, the prepared films of each sample were then thoroughly washed with acetone, blown dry with nitrogen at room temperature, and then dried in an oven at 80°C for 24 h.

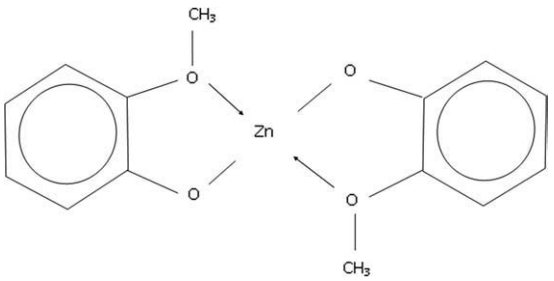

Figure 1 Dimeric bonds formed between a zinc ion and two guaiacol molecules.

The crystal structure and morphology of the prepared ZnO film on the surface of the wood substrates were characterized with XRD (Philips, PW 1840 diffractometer), FTIR spectroscopy (Varian Instruments, Walnut Creek, CA), TGA (TA Instruments, New Castle, DE), and SEM (FEI QUANTA200, Hillsboro, OR). The wettability of each sample was evaluated by the measurement of the water contact angle at the sample surfaces with a goniometer (Hitachi High-Tech, Minato-Ku, Tokyo, Japan). The water contact angles of each sample were evaluated on the early wood and late wood surfaces.

RESULTS AND DISCUSSION

To grow ZnO nanorods on the surface of wood, it was necessary to chemically seed ZnO molecules on the cell walls. It has been found that Zn^{2+} forms insoluble complexes with guaiacol groups of lignin through dimeric bonds, which are stronger than the wood–water bond.[4,15] Figure 1 shows the dimeric bonds between two guaiacol groups and one Zn^{2+} cation. Therefore, the chemically seeded ZnO molecules were insoluble and could not be leached out by the water solutions. After they are deposited on the surface of wood, ZnO molecular seeds may grow into nanorods when free ZnO molecules are available in the solution. The deposition reaction of ZnO molecules can be expressed as follows:[16,17]

$$Zn^{2+} + CO(NH_2)_2 + 2H_2O \rightarrow ZnO + CO_2 + 2NH_4^+. \quad (1)$$

The reaction is continuous and is controllable by the pH of the solution. Nanorod sizes and shapes are strongly dependent on the number of OH^- groups or the pH values of the solutions. When the OH^- concentration in the solution is higher than the stoichiometric concentration, single-crystal nanorods are produced; when the OH^- concentration in the

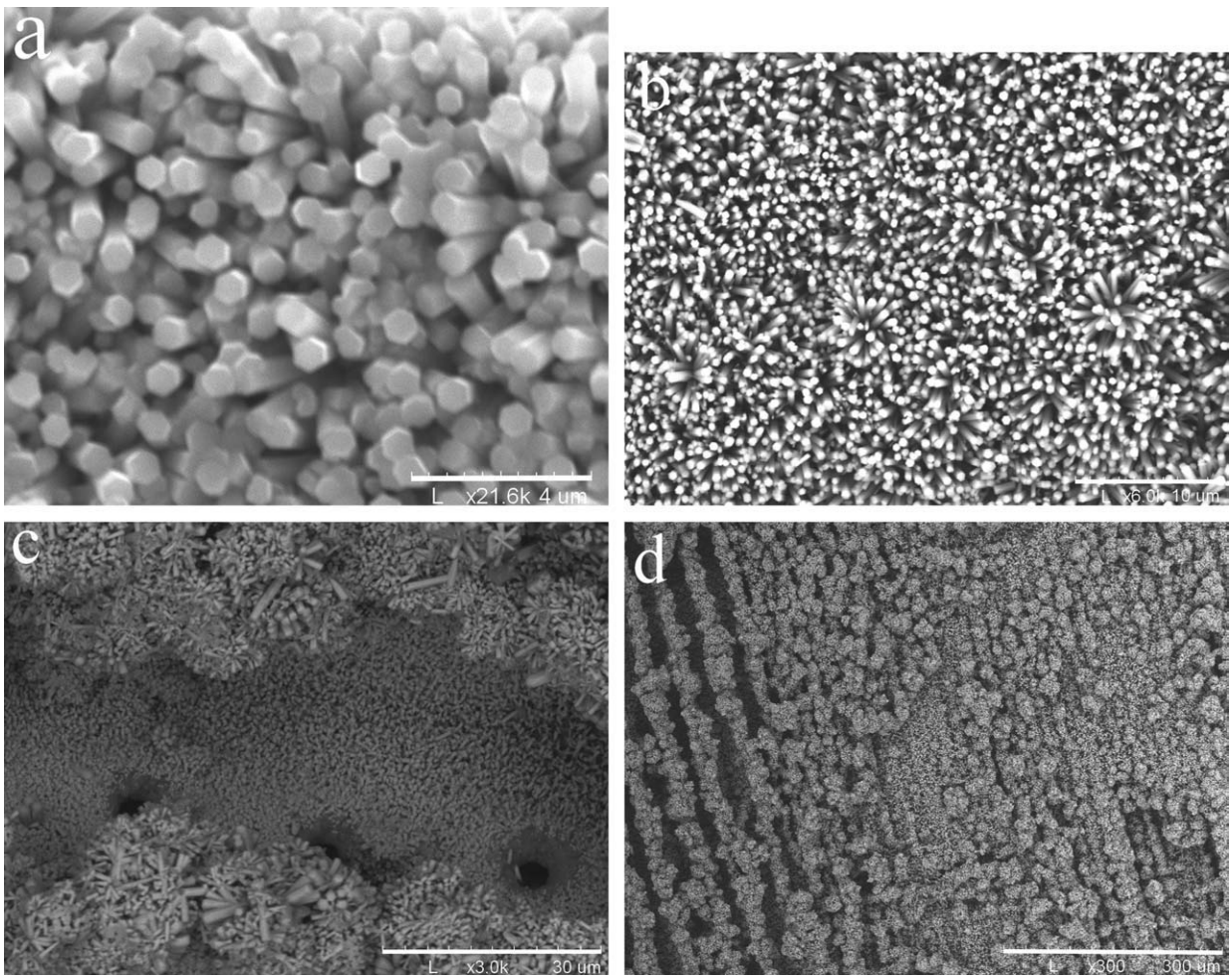

Figure 2 SEM images of the prepared ZnO films on the wood substrates: (a) hexagonal nanorods of ZnO crystals, (b) the ZnO nanofilm on the wood substrate, (c) top-layer growth near the cross-sectional wall areas (top and bottom) and bottom-layer growth at the inner lumenal surface and around the pit apertures (center), and (d) ZnO growth in the early wood (left) and late wood areas (right).

solution is lower than the stoichiometric concentration, polycrystalline nanorods are produced.[18] A high solution pH allows the production of slender nanorods, which are necessary to form microscale and nanoscale roughnesses on a substrate surface. The diameter of the nanorods decreased with increasing pH value of the solution. The pH values used for the superhydrophobic surface coating of wood were greater than the stoichiometric concentration.

Figure 2 shows the SEM images of the prepared ZnO nanofilms on the surface of the wood substrates, from which we observed that the ZnO nanorods formed a dense forest on the surface of the wood [Fig. 2(a,b)]. The rods had diameters ranging from 300 to 600 nm and lengths of about 1 μm. Figure 2(a) shows the hexagonal structure of the ZnO nanorods.

In the formation of nanorods, ZnO molecules were first deposited on the wood surface by dimeric bonds with the guaiacol groups on wood cell walls to form a seeded layer. Figure 3 illustrates the distribution of ZnO nanoseeds on the surface of cell walls after 5 h of reaction. ZnO seeds adsorbed more to the cross-sectional walls than to the inner lumenal surface because of the presence of more lignin, and the corresponding greater presence of guaiacol groups in the primary wall and middle lamella. Figure 2(c) also illustrates that ZnO nanorods were more numerous on the cross-sectional walls than on the inner lumenal surfaces at the end of the reaction. Therefore, differential growth occurred between the cross-sectional wall and inner lumenal surface; this led to a layering structure near the cross-sectional wall areas. The top layer consisted of flower-shaped larger nanorods on the cross-sectional walls; below the top layer were found smaller, more tightly arranged rods forming a smoother surface on the inner lumenal surface. The space between the tightly arranged nanorods shown in Figure 2(a–c) constituted the nanoscale roughness.

Figure 2(c) also shows that the pits or outer apertures of the wood were not covered by the ZnO nanorods. *Pit spots* are thin areas in the cell wall that

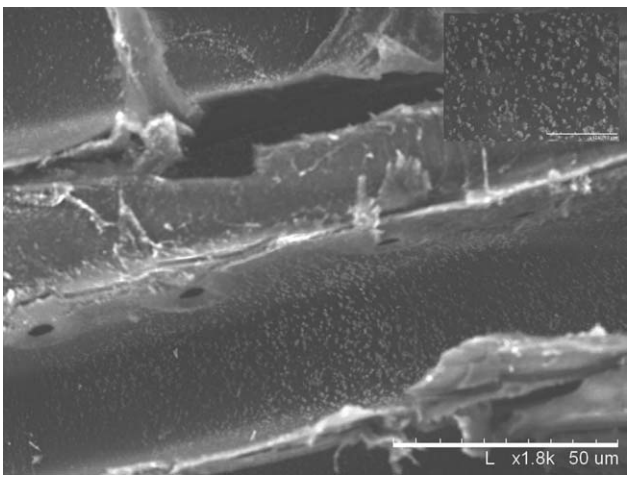

Figure 3 ZnO nanoseeds on the surface of the cell walls (reaction time = 5 h).

are readily penetrated by the treatment solution. In such areas, ZnO nanorods grew on the surfaces of the inner lumenal cell walls directly below the wood surface. As mentioned previously, the average radius of a tracheid was 17–60 μm, and the average radii of the fiber and vessel were 10–30 and 20–350 μm, respectively.[1] With regard to the length of a typical nanorod (1 μm), spaces in the lumens were available for the growth of the nanorods in the lumens below the surface layer. However, depending on the pressure, the nanogrowth tended to diminish for deeper lumens in the wood because the mobility of the solution decreased with increasing penetration depth. When ZnO molecules were exhausted in the deep regions, a deficiency of ZnO in the solution persisted due to the lack of mobility of the solution in such regions. To increase mobility, cyclic vacuum and pressure were applied during the nanorod growing process. We will discuss the results of the ZnO nanorod growth *in vacuo* and the pressure conditions in our next publication.

Figure 2(d) shows a microview of the ZnO nanorod distributions on the cell walls. ZnO nanorods grew along cross-sectional cell walls and on the concave inner lumenal surfaces. The nanorods did not fill out the lumenal cavities in the early wood. Therefore, the coated surface appeared differently according to surface roughness, that is, the rougher early wood and the smoother late wood regimes.

Figure 4 illustrates four wetting regimes. According to Wenzel,[19] the true wetting area of a rough, nonideal surface is greater than its nominal (or geometrical) area, and the wetting properties of the surface are directly proportional to the roughness of the surface. Roughness enhances both the hydrophilicity and hydrophobicity of a surface. For a hydrophobic wood surface (contact angle $> 90°$), the apparent contact angle of the coated surface is greater than the contact angle of the uncoated cell wall. It was evident that the total roughness of the prepared wood surface consisted of the roughness due to the nanorod forest and the roughness due to the cell wall topography (cross-sectional walls and lumenal cavities). Because the prepared surface was hydrophobic, the surface of the dense nanoforest areas (on the inner lumenal surface), shown in Figure 2(a,b), was believed to conform to the Cassie–Baxter wetting models, whereas the roughness due to the cell wall topography, shown in Figure 2(c,d), was believed to conform to the superhydrophobic porous wetting model.

Therefore, the ZnO nanorod structure was superhydrophobic after the nanorod surfaces were modified by alkanoic acids through the SAM process. Figure 4 shows water droplets on the surfaces of uncoated and ZnO-coated wood substrates. The uncoated wood surface had a water contact angle of 57°. After hydrophobic modification, the coated wood surface showed a water contact angle of up to 153.5°. The early wood surface showed an average water contact angle of 150°, and the late wood surface showed an average water contact angle of 146°. Therefore, the surface tension of the coated early wood was less than the surface tension of the coated late wood, likely because the early wood surface was rougher than the late wood surface. The differential surface characteristics of superhydrophobic early wood and late wood will be evaluated further in future studies.

The XRD pattern of the ZnO nanostructures grown on the wood substrate was similar to the wurtzite hexagonal structure (Jointed Committee on

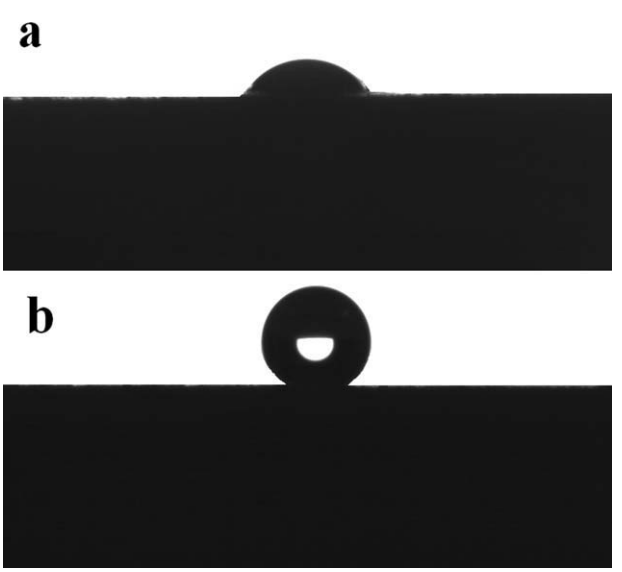

Figure 4 Water droplets were placed on (a) original, uncoated southern pine wood surfaces and (b) modified southern pine wood surfaces modified by ZnO nanorods and stearic acid.

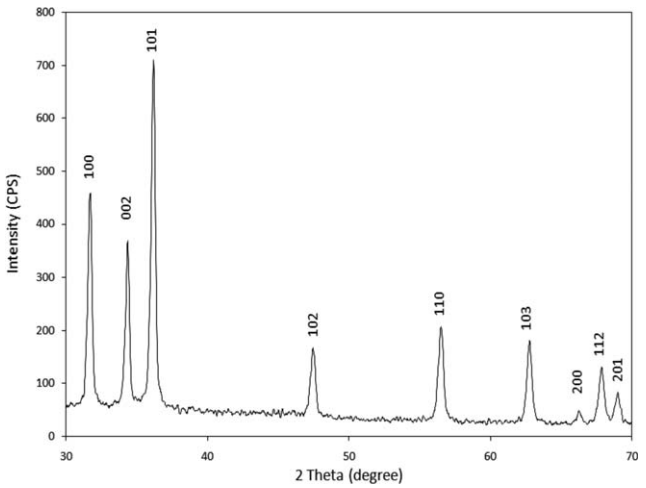

Figure 5 XRD pattern of the prepared ZnO nanorods on a wood surface.

Powder Diffraction Standards card number 36–1451) with lattice constants of a =.325 nm and c =.521 nm (Fig. 5). No additional peaks were observed in the ZnO film on the wood substrates.

The FTIR spectra of the pure stearic acid and the ZnO film modified by stearic acid on the wood surfaces both showed two strong peaks, one at 2916 cm^{-1} and the other at 2847 cm^{-1} (Fig. 6), which represented CH_3 and CH_2 stretching, respectively, and indicated that stearic acid was attached to the ZnO–wood surface. The 1699-cm^{-1} peak, produced by C=O stretching, was found in the spectrum of stearic acid, but the same peak was not found in the spectrum of the ZnO–wood surface modified by stearic acid. In addition, a comparison between the spectrum of wood–ZnO–stearic acid and the spectrum of wood–ZnO showed several new peaks, including peaks at 1540 and 1453 cm^{-1}, which represented the asymmetric and symmetric stretching of carboxylate ions.[20] The differential asymmetric and symmetric stretching induced the adsorption of stearic acid ions to the surface of the ZnO nanorods. Pinprayoon et al.[21] found that Zn^{2+} ions formed ionic crosslinks with carboxylate groups. Therefore, it was possible that stearic acid molecules were attached to the ZnO nanorods by single-molecular-layer adsorption through the SAM process.

The FTIR spectra of both ZnO–wood and ZnO–wood modified by stearic acid did not show absorption bands at 1330 and 1260 cm^{-1} (Fig. 6), which were the stretching of OH coupled to C=C stretching of the aromatic ring (lignin at 1330 cm^{-1}) and the absorption band of phenol (1260 cm^{-1}).[4] Both peaks featured the absorption bands of the guaiacol groups. The disappearance of the two characteristic peaks of the guaiacol groups (1330 and 1260 cm^{-1}) from the wood–ZnO and wood–ZnO–steric acid spectra was primarily due to the formation of the dimeric bonds between zinc cations and guaiacol groups of lignin at the surface of wood (Fig. 1). Therefore, before and after the modification with stearic acid, ZnO nanorods were likely chemically bonded to the wood surface by dimeric bonds.

The TGA curves of the hydrophobically treated and untreated wood in nitrogen showed a 4% weight reduction from ambient temperature (25°C) to 180°C (Fig. 7). Moisture and, to a lesser extent, volatile organic compounds in both the treated and untreated wood samples were evaporated by heat during this period. Because the treated wood samples were soaked in the basic and hexane solutions, most VOCs were likely extracted by the basic and hexane solutions during the hydrophobic treatment. Thus, the weight reduction in the treated wood samples was predominantly due to the loss of water, which comprised 4% of the total sample weight. The thermal decomposition of the untreated wood

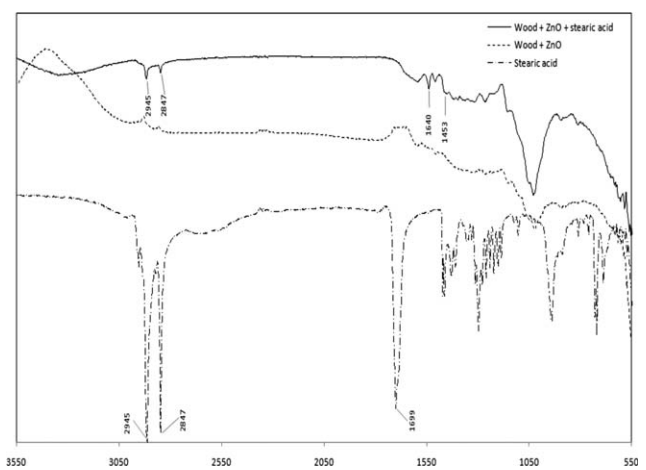

Figure 6 FTIR spectra of stearic acid, a wood surface coated with ZnO nanorods, and a wood surface coated with ZnO nanorods and stearic acid.

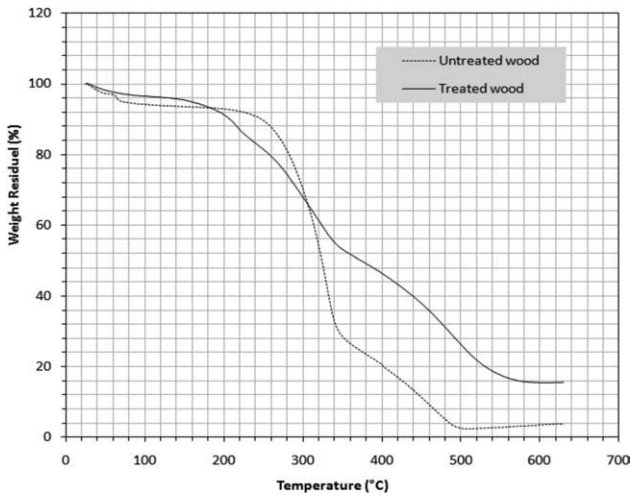

Figure 7 Weight residuals of hydrophobically treated and untreated southern pine wood.

occurred from 220 to 500°C, whereas the thermal decomposition of the treated wood occurred from 180 to 560°C; this showed that treated wood decomposed earlier but more slowly than the untreated wood. The initial and final decomposition temperature differences between the treated and untreated wood were likely due to the higher content of lignin in the treated wood. Lignin often decomposes earlier but much more slowly than cellulose.[22] Because of the hydrolysis of the cellulose and hemicellulose components in the basic treatment solution, the treated wood surface had a higher lignin content than the untreated wood surface.

CONCLUSIONS

Superhydrophobic surfaces were developed on wood substrates by the cultivation of ZnO nanorods on the wood surface and the subsequent modification of the ZnO nanorod surfaces with stearic acid. The roughness of the coated wood surface was consistent with the Cassie–Baxter wetting regime for inner lumenal areas and the hydrophobic porous wetting regime for other areas. The contact angle of the coated surface was up to 153.5°. The contact angles were greater for the early wood surface than for the late wood surface because the coated early wood surface was rougher than that of the late wood. The early seeding of ZnO nanoparticles on the cross-sectional walls led to a layering structure in the ZnO nanofilms. Larger and flower-shaped nanorods were found on the cross-sectional walls, and smaller, vertically arranged nanorods were found on the inner lumenal surfaces. The spaces between nanorods constituted the nanoscale roughness of the superhydrophobic surface, whereas the microroughness of wood surface constituted the microroughness of the superhydrophobic surface. The results of XRD, TGA, and FTIR spectroscopy showed that hexagonal ZnO nanorods could be seeded and grown on the cell wall surfaces of wood. Superhydrophobic surfaces can be developed on wood substrates by the modification of the ZnO nanorods with SAMs of stearic acid.

The authors thank Semi Nazzal, College of Pharmacy, University of Louisiana at Monroe, Louisiana; George Grozdits and Mark Gibson, School of Forestry, Louisiana Tech, Ruston, Louisiana; Jian Wang, School of Plan, Environmental and Soil Sciences, Louisiana State University Agricultural Center, Baton Rouge, Louisiana; and Neal Hickman, Calhoun Research Station, Louisiana State University Agricultural Center, Calhoun, Louisiana, for their assistance in this study. This research was funded by and conducted at the Calhoun Research Station, Louisiana State University Agricultural Center. This article (2010-255-6068) was published with the approval of the Director of the Louisiana Agricultural Experiment Station.

References

1. Bodig, J.; Jayne, B. A. Mechanics of Wood and Wood Composites; Krieger: Melbourne, FL, 1993; p 736.
2. Marmur, A. Annu Rev Mater Res 2009, 39, 473.
3. Rowell, R. M. Forest Prod J 2006, 56, 9, 4.
4. Kubel, H.; Pizzi, A. J. Wood Chem Technol 1981, 1, 1, 75.
5. Saka, S.; Ueno, T. Wood Sci Technol 1997, 31, 457.
6. Tshabalala, M. A.; Kinshott, P.; VanLandingham, M. R.; Plackett, D. J Appl Polym Sci 2003, 88, 2828.
7. Donath, S.; Militz, H.; Mai, C. Wood Sci Technol 2004, 38, 555.
8. Ghosh, S. C.; Militz, H.; Mai, C. Eur J Wood Prod 2009, 67, 159.
9. Bente, M.; Avramidis, G.; Forster, S.; Rohwer, E. G. Holz Roh Werkst 2004, 62, 157.
10. Yang, H. Fundamentals, preparation, and characterization of superhydrophobic wood fiber products; Thesis, School of Chemical and Biomolecular Engineering, Georgia Institute of Technology: Atlanta, GA, 2008; p 83.
11. Xue, C.-H.; Jia, S.-T.; Chen, H.-Z.; Wang, M. Sci Technol Adv Mater 2008, 9, 1.
12. Li, S.; Zhang, S.; Wang, X. Langmuir 2008, 24, 5585.
13. Sebe, G.; Brook, M. A. Wood Sci Technol 2001, 35, 269.
14. Artus, G. R. J.; Jung, S.; Zimmermann, J.; Gautschi, H.-P.; Marquardt, K.; Seeger, S. Adv Mater 2006, 20, 2758.
15. Nanassy, A. J.; Desai, R. L. Wood Sci 1978, 10, 204.
16. Tsuchida, T.; Kitajima, S. Chem Lett 1990, 19, 1769.
17. Ledwith, D.; Pillai, S. C.; Watson, G. W.; Kelly, J. M. Chem Commun 2004, 20, 2294.
18. Ullah, M. D. H.; Kim, I.; Ha, C.-S. J Mater Sci 2006, 41, 3263.
19. Wenzel, R. N. Ind Eng Chem 1936, 28, 988.
20. Wu, X.; Zheng, L.; Wu, D. Langmuir 2005, 21, 2665.
21. Pinprayoon, O.; Saiani, A.; Groves, R.; Saunders, B. R. J Colloid Interface Sci 2009, 336, 73.
22. Lee, H.-L.; Chen, G. C.; Rowell, R. M. J Appl Polym Sci 2004, 91, 2465.